The dependence of the galaxy luminosity function on large-scale environment

H. J. Mo,[1][*] Xiaohu Yang,[1,2] Frank C. van den Bosch[3,4] and Y. P. Jing[5]

[1]*Department of Astronomy, University of Massachusetts, Amherst MA 01003-9305, USA*
[2]*Center for Astrophysics, University of Science and Technology of China, Hefei, Anhui 230026, China*
[3]*Institute of Astronomy, Swiss Federal Institute of Technology, ETH Hönggerberg, CH-8093, Zurich, Switzerland*
[4]*Max-Planck-Institut für Astrophysik, Karl-Schwarzschild-Strasse 1, 85748 Garching, Germany*
[5]*Shanghai Astronomical Observatory; the Partner Group of MPA, Nandan Road 80, Shanghai 200030, China*

ABSTRACT

A basic assumption in the current halo-occupation model is that the properties of a galaxy depend only on the mass of its dark matter halo. An important consequence of this is that the segregation of the galaxy population by large-scale environment is entirely due to the environmental dependence of the halo population. In this paper, we use such a model to predict how the galaxy luminosity function depends on large-scale environment. The latter is represented by the density contrast (δ) averaged over a spherical volume of radius $R = 8\ h^{-1}$ Mpc. The model predicts that the Schechter function is a good approximation to the luminosity functions of galaxies brighter than $\sim 10^9\ h^{-2}\ L_\odot$ (b_J-band) in virtually all environments. The characteristic luminosity, $L^\star$, increases moderately with δ. The faint-end slope, α, on the other hand, is quite independent of δ. However, when splitting the galaxy population into early and late types, it is found that for late types, α is virtually constant, whereas for early types, α increases from ~ -0.3 in underdense regions ($\delta \sim -0.5$) to ~ -0.8 in highly overdense regions ($\delta \sim 10$). The luminosity function at $L_{b_J} < 10^9\ h^{-2}\ L_\odot$ is significantly steeper than the extrapolation of the Schechter function that fits the brighter galaxies. This steepening is more significant for early types and in low-density environments. The model also predicts that the luminosity density and the mass density are closely correlated. The relation between the two is monotonic but highly non-linear. This suggests that one can use the luminosity density, averaged over a large volume, to rank the mass density. This, in turn, allows the environmental effects predicted here to be tested by observations.

Key words: methods: statistical – galaxies: haloes – dark matter – large-scale structure of Universe.

1 INTRODUCTION

In a hierarchical cosmogony like the cold dark matter (CDM) model, galaxies are assumed to form in dark matter haloes (e.g. White & Rees 1978). A generic prediction of such a cosmogony is that the properties of the galaxy population must be closely related to that of the halo population. If the cosmological density field is Gaussian and if the power of density perturbations extends to large scales, as is the case in the current CDM cosmogony, halo properties are expected to be correlated to some degree with the large-scale structure, and so the properties of the galaxy population are also expected to change with large-scale environment. With high-resolution numerical simulations, much has been learned about the halo population. It turns

out that a strong correlation with the large-scale environment exists only for halo mass; all other important halo properties are at most weakly correlated with the large-scale environment at any given time (e.g. Lemson & Kauffmann 1999). This result, combined with our current model of galaxy formation, implies that the environmental dependence of the galaxy population is mainly due to the change in the halo mass function with large-scale environment. We can therefore hope to understand the environmental dependence of the galaxy population by understanding how galaxies occupy dark haloes of different masses. This is indeed the approach taken by the so-called halo-occupation models, in which the *number* of galaxies per halo is assumed to depend on halo *mass* only (e.g. Jing, Mo & Börner 1998; Peacock & Smith 2000; Seljak 2000; Benson 2001; Scoccimarro et al. 2001; Berlind & Weinberg 2002; Bullock, Wechsler & Somerville 2002; Kang et al. 2002; Scranton 2002; Zheng et al. 2002; Kravtsov et al. 2003; Magliocchetti & Porciani 2003;

[*]E-mail: hjmo@nova.astro.umass.edu

van den Bosch, Yang & Mo 2003a; Yan, Madgwick & White 2003; Yang, Mo & van den Bosch 2003a; Zehavi et al. 2003). Note that this assumption is non-trivial, as it implies that galaxy formation is largely a local process in individual dark matter haloes. This assumption was also made in many of the semi-analytic models based on Monte Carlo halo merging trees (e.g. Kauffmann, White & Guiderdoni 1993; Cole et al. 1994; Sommerville & Primark 1999), because in such models, the merging histories are statistically the same for all haloes of the same mass at a given time. Berlind et al. (2003) found that this assumption is consistent with their numerical simulations.

To test the validity of this assumption, we use the halo-occupation model recently developed by Yang et al. (2003a), which is based on the conditional luminosity function (hereafter CLF) of galaxies in dark haloes of given mass, to predict how the galaxy luminosity function (hereafter LF) changes with large-scale environment. In this model, the change of the LF with large-scale environment is entirely due to the change of the halo mass function with large-scale environment. Because the conditional mass function of dark matter haloes can be accurately obtained from cosmological N-body simulation, the CLF model can be used to make accurate predictions for how the galaxy LF changes with large-scale density field. We also show that, when averaged over a large volume, the predicted galaxy luminosity density is closely correlated with the underlying mass density. Therefore, the luminosity density can be used to rank the mass density, and the model predictions presented here can be tested using large galaxy redshift surveys, such as the two-degree Field Galaxy Redshift Survey (2dFGRS; Colless et al. 2001) and the Sloan Digital Sky Survey (SDSS; York et al. 2000).

The paper is arranged as follows. In Section 2, we review the CLF model and describe how it can be used to calculate the LF of galaxies in different environments. Section 3 presents the model predictions for how the galaxy LF changes with large-scale density field. In Section 4, we use our model to study the correlation between the galaxy luminosity density and the underlying mass density, and discuss how the predictions of our CLF formalism can be tested with observations. We summarize our results in Section 5.

2 FROM THE CONDITIONAL LUMINOSITY FUNCTION TO THE GALAXY LUMINOSITY FUNCTION

In Yang et al. (2003a, hereafter Paper I), we developed a formalism, based on the conditional LF $\Phi(L\,|\,M)$, to link the distribution of galaxies to that of dark matter haloes. We introduced a parametrized form for $\Phi(L\,|\,M)$, which we constrained using the LF and the correlation lengths as function of luminosity. In van den Bosch, Yang & Mo (2003a, hereafter Paper II), we extended our model by constructing separate CLFs for the early- and late-type galaxies. The CLF formalism developed in these two papers has subsequently been used to investigate galaxy clustering as function of luminosity and type (Yang et al. 2003b), to put constraints on cosmological parameters (van den Bosch, Mo & Yang 2003b), to constrain redshift-evolution in the halo model (Yan et al. 2003) and to characterize the population of satellite galaxies (van den Bosch et al., in preparation). In this paper, we use the CLF formalism to predict how the LF of galaxies depends on large-scale environment. For completeness, we briefly summarize in the following the main ingredients of the CLF formalism, and we refer the reader to Papers I and II for more details.

The conditional LF $\Phi(L\,|\,M)\,\mathrm{d}L$ gives the average number of galaxies with luminosities in the range $L \pm \mathrm{d}L/2$ that reside in

haloes of mass M. It is parametrized by a Schechter function:

$$\Phi(L\,|\,M)\,\mathrm{d}L = \frac{\tilde{\Phi}^*}{\tilde{L}^*}\left(\frac{L}{\tilde{L}^*}\right)^{\tilde{\alpha}}\exp(-L/\tilde{L}^*)\,\mathrm{d}L, \qquad (1)$$

where $\tilde{L}^* = \tilde{L}^*(M)$, $\tilde{\alpha} = \tilde{\alpha}(M)$ and $\tilde{\Phi}^* = \tilde{\Phi}^*(M)$ are all functions of halo mass M. Following Papers I and II, we write the average total mass-to-light ratio of a halo with mass M as

$$\left\langle\frac{M}{L}\right\rangle(M) = \frac{1}{2}\left(\frac{M}{L}\right)_0\left[\left(\frac{M}{M_1}\right)^{-\gamma_1} + \left(\frac{M}{M_1}\right)^{\gamma_2}\right], \qquad (2)$$

which has four free parameters: a characteristic mass M_1, for which the mass-to-light ratio is equal to $(M/L)_0$, and two slopes, γ_1 and γ_2, that specify the behaviour of $\langle M/L\rangle$ at the low- and high-mass ends, respectively. A similar parametrization is adopted for the characteristic luminosity $\tilde{L}^*(M)$:

$$\frac{M}{\tilde{L}^*(M)} = \frac{1}{2}\left(\frac{M}{L}\right)_0 f(\tilde{\alpha})\left[\left(\frac{M}{M_1}\right)^{-\gamma_1} + \left(\frac{M}{M_2}\right)^{\gamma_3}\right], \qquad (3)$$

with

$$f(\tilde{\alpha}) = \frac{\Gamma(\tilde{\alpha}+2)}{\Gamma(\tilde{\alpha}+1,1)}. \qquad (4)$$

Here $\Gamma(x)$ is the Gamma function and $\Gamma(a, x)$ the incomplete Gamma function. This parametrization has two additional free parameters: a characteristic mass M_2 and a power-law slope γ_3. For $\tilde{\alpha}(M)$, we adopt a simple linear function of $\log(M)$,

$$\tilde{\alpha}(M) = \alpha_{15} + \eta\log(M_{15}), \qquad (5)$$

with M_{15} the halo mass in units of $10^{15}\,h^{-1}\,\mathrm{M}_\odot$, $\alpha_{15} = \tilde{\alpha}(M_{15} = 1)$, and η describes the change of the faint-end slope $\tilde{\alpha}$ with halo mass. Note that once $\tilde{\alpha}(M)$ and $\tilde{L}^*(M)$ are given, the normalization of the CLF, $\tilde{\Phi}^*(M)$, is obtained through equations (1) and (2), using the fact that the total (average) luminosity in a halo of mass M is

$$\langle L\rangle(M) = \int_0^\infty \Phi(L\,|\,M)L\,\mathrm{d}L = \tilde{\Phi}^*\tilde{L}^*\Gamma(\tilde{\alpha}+2). \qquad (6)$$

Finally, we introduce the mass scale M_{min} below which we set the CLF to zero; i.e., we assume that no stars form inside haloes with $M < M_{\mathrm{min}}$. Motivated by reionization considerations (see Paper I for details), we adopt $M_{\mathrm{min}} = 10^9\,h^{-1}\,\mathrm{M}_\odot$ throughout.

In order to split the galaxy population into early and late types, we follow Paper II and introduce the function $f_{\mathrm{late}}(L, M)$, which specifies the fraction of galaxies with luminosity L in haloes of mass M that are late-type. The CLFs of late- and early-type galaxies are then given by

$$\Phi_{\mathrm{late}}(L\,|\,M)\,\mathrm{d}L = f_{\mathrm{late}}(L, M)\Phi(L\,|\,M)\,\mathrm{d}L \qquad (7)$$

and

$$\Phi_{\mathrm{early}}(L\,|\,M)\,\mathrm{d}L = [1 - f_{\mathrm{late}}(L, M)]\,\Phi(L\,|\,M)\,\mathrm{d}L. \qquad (8)$$

As with the CLF for the entire population of galaxies, $\Phi_{\mathrm{late}}(L\,|\,M)$ and $\Phi_{\mathrm{early}}(L\,|\,M)$ are constrained by 2dFGRS measurements of the LFs and the correlation lengths as function of luminosity. We assume that $f_{\mathrm{late}}(L, M)$ has a quasi-separable form

$$f_{\mathrm{late}}(L, M) = g(L)h(M)q(L, M). \qquad (9)$$

Here,

$$q(L, M) = \begin{cases} 1 & \text{if } g(L)h(M) \leqslant 1 \\ \dfrac{1}{g(L)h(M)} & \text{if } g(L)h(M) > 1 \end{cases} \qquad (10)$$

is to ensure that $f_{\text{late}}(L, M) \leqslant 1$. We adopt

$$g(L) = \frac{\hat{\Phi}_{\text{late}}(L)}{\hat{\Phi}(L)} \frac{\int_0^\infty \Phi(L \mid M) n(M) \, \mathrm{d}M}{\int_0^\infty \Phi(L \mid M) h(M) n(M) \, \mathrm{d}M}, \tag{11}$$

where $n(M)$ is the halo mass function (Sheth & Tormen 1999; Sheth, Mo & Tormen 2001), $\hat{\Phi}_{\text{late}}(L)$ and $\hat{\Phi}(L)$ correspond to the *observed* LFs of the late-type and entire galaxy samples, respectively, and

$$h(M) = \max \left\{ 0, \min \left[1, \left(\frac{\log(M/M_a)}{\log(M_b/M_a)} \right) \right] \right\}, \tag{12}$$

with M_a and M_b two additional free parameters, defined as the masses at which $h(M)$ takes on the values 0 and 1, respectively. As shown in Paper II, this parametrization allows the population of galaxies to be split in early- and late-types such that their respective LFs and clustering properties are well fitted.

In Papers I and II, we presented a number of different CLFs for different cosmologies and different assumptions regarding the free parameters. In what follows, we focus on the flat ΛCDM cosmology with $\Omega_{\text{m}} = 0.3$, $\Omega_\Lambda = 0.7$ and $h = H_0/(100 \text{ km s}^{-1} \text{ Mpc}^{-1}) = 0.7$, and with initial density fluctuations described by a scale-invariant power spectrum with normalization $\sigma_8 = 0.9$. These cosmological parameters are in good agreement with a wide range of observations, including the recent *Wilkinson Microwave Anisotropy Probe* (*WMAP*) results (Spergel et al. 2003); in what follows, we refer to it as the 'concordance' cosmology. Finally, we adopt the CLF with the following parameters: $M_1 = 10^{10.94} \, h^{-1} \, \text{M}_\odot$, $M_2 = 10^{12.04} \, h^{-1} \, \text{M}_\odot$, $M_a = 10^{17.26} \, h^{-1} \, \text{M}_\odot$, $M_b = 10^{10.86} \, h^{-1} \, \text{M}_\odot$, $(M/L)_0 = 124 \, h \, (\text{M/L})_\odot$, $\gamma_1 = 2.02$, $\gamma_2 = 0.30$, $\gamma_3 = 0.72$, $\eta = -0.22$ and $\alpha_{15} = -1.10$. As shown in paper II, this model (referred to as model D) yields excellent fits to the observed LFs and the observed correlation lengths as function of both luminosity and type. We emphasize, however, that our results are not sensitive to uncertainties in the CLF; had we chosen models A, B or C in paper II, instead of model D, the results presented below would have been virtually identical. Because $\Phi(L \mid M)$ is the average number of galaxies per unit luminosity in a halo with mass M, one can obtain the galaxy LF, $\Phi(L)$, from the halo mass function, $n(M)$, according to

$$\Phi(L) = \int \Phi(L \mid M) n(M) \, \mathrm{d}M. \tag{13}$$

Fig. 1 shows how haloes of different masses contribute to the total LF. Note that the shape of the CLF changes significantly with halo mass, and that the faint end of the LF is dominated by galaxies hosted by low-mass haloes.

If we make the assumption that the CLF is statistically independent of the large-scale environment, the galaxy LF in a region of overdensity δ follows from

$$\Phi(L \mid \delta) = \int \Phi(L \mid M) n(M \mid \delta) \, \mathrm{d}M. \tag{14}$$

Here, $n(M \mid \delta)$ is the conditional mass function of dark matter haloes, which gives the number density of haloes as a function of halo mass in an environment with average mass overdensity $\delta \equiv [\mathcal{M} - \overline{\mathcal{M}}]/\overline{\mathcal{M}}$ (with $\mathcal{M}$ the total mass in volume V, and $\overline{\mathcal{M}}$ the mean mass in all volumes V). Thus, in the CLF formalism, the δ-dependence of the galaxy LF enters only though the conditional mass function $n(M \mid \delta)$.

Fig. 2 shows the conditional mass functions for haloes in several representative environments. These functions are derived from a high-resolution N-body simulation which follows the motions of 512^3 particles with a P^3M code in a $100 \, h^{-1}$ Mpc box (see Jing & Suto 2002, for details), assuming the ΛCDM 'concordance' cosmology specified above. Dark matter haloes are identified using the
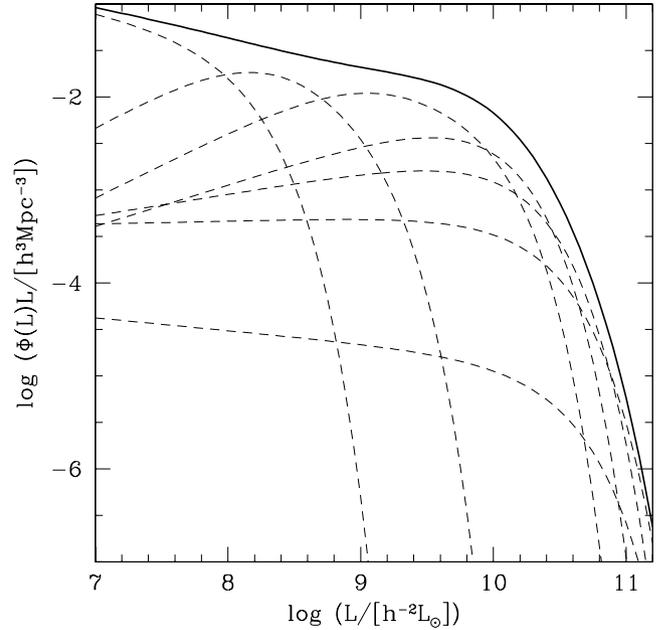

Figure 1. The contribution to the total LF (solid curve) by haloes in various mass ranges: $M/[h^{-1} \, \text{M}_\odot] \leqslant 5 \times 10^{10}$, 5×10^{10}–10^{11}, 10^{11}–10^{12}, 10^{12}–10^{13}, 10^{13}–10^{14}, 10^{14}–10^{15} and $> 10^{15}$ (broader curve corresponds to larger mass).

standard friends-of-friends algorithm with a linking length of 0.2 times the mean interparticle separation. As one can see, the shape of the conditional mass function is quite independent of δ at the low-mass end, whereas the shape at the high-mass end depends significantly on δ. The break in the conditional mass function at the high-mass end occurs at a lower mass for lower δ. This reflects the fact that the formation of massive haloes is suppressed in low-density regions due to bias (e.g. Mo & White 1996; Gottloeber et al. 2003). For a given δ, the break occurs at smaller mass if the volume used to define δ is smaller.

Ideally, if we have an accurate model for the conditional mass function, we can combine it with the CLF to construct an analytical model for the δ-dependence of the galaxy LF. Unfortunately, the model based on peak-background splitting (e.g. Cole & Kaiser 1989; Mo & White 1996) is not sufficiently accurate for our purpose, even if ellipsoidal collapse is taken into account (Sheth et al. 2001; Sheth & Tormen 2002). The reason for this is that, when the total mass contained in a volume becomes comparable to the mass of individual haloes in consideration, as is the case for massive haloes in low-density volumes, the peak-background splitting becomes inaccurate (e.g. Sheth & Tormen 2002). We therefore decided to use the simulated samples constructed in Yang et al. (2003b) for our purpose. These simulated samples were obtained by populating dark matter haloes in N-body simulations with galaxies according to the CLF model described above. Here, we use the sample constructed from one of the $100 \, h^{-1}$ Mpc simulations, which is complete down to a b_J-band luminosity of $L_{b_J} \sim 10^8 \, h^{-2} \, \text{L}_\odot$ (see Yang et al. 2003b for details).

3 GALAXY LUMINOSITY FUNCTION IN DIFFERENT ENVIRONMENTS

Fig. 3 shows the LFs of galaxies in regions of different mass overdensities δ (defined over spheres with radius $R = 8 \, h^{-1}$ Mpc). As one
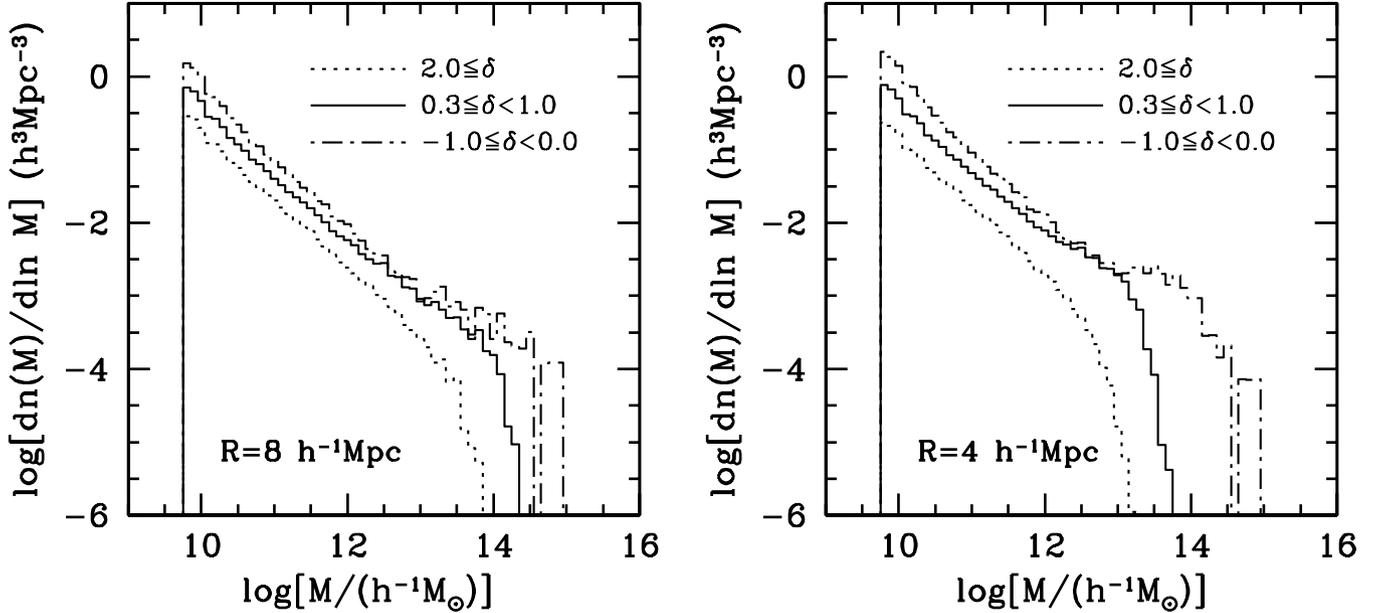
Figure 2. The conditional mass functions of dark matter haloes in various environments, specified by the mass overdensity δ in a spherical volume with radius $R = 8\ h^{-1}$ Mpc (left-hand panel) and $R = 4\ h^{-1}$ Mpc (right-hand panel).
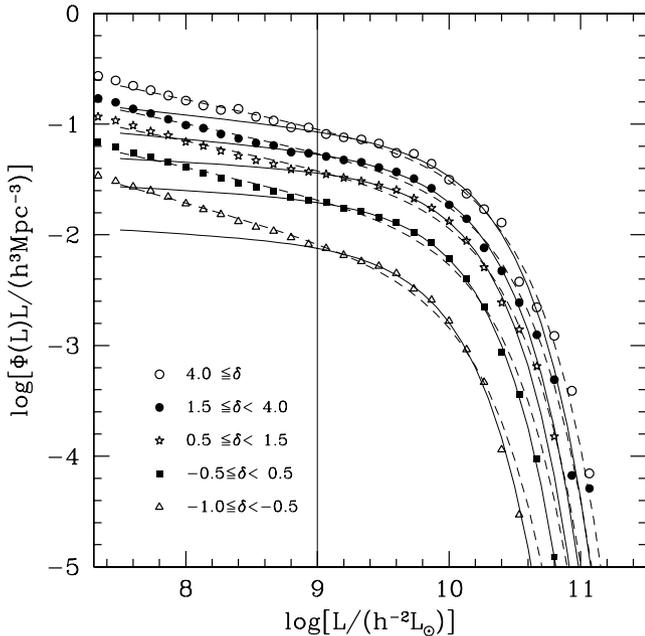

Figure 3. Galaxy LFs in regions with different mass overdensities: $-1.0 \leqslant \delta < -0.5$ (open triangles), $-0.5 \leqslant \delta < 0.5$ (solid squares), $0.5 \leqslant \delta < 1.5$ (asterisks), $1.5 \leqslant \delta < 4.0$ (solid circles) and $\delta \geqslant 4.0$ (open circles). The solid and dashed curves correspond to the best-fitting Schechter functions, fit over the luminosity ranges $L_{b_J} \geqslant 10^9\ h^{-2}$ $L_\odot$ and $L_{b_J} \geqslant 10^{7.5}\ h^{-2}$ $L_\odot$, respectively.

can see, the *shape* of the LF at the faint end is quite independent of δ. This is due to the fact that most faint galaxies reside in low-mass haloes, for which the *shape* of the conditional mass function $n(M \mid \delta)$ is only weakly dependent on δ (cf. Fig. 2). The most pronounced difference between LFs in different mass density environments is the break at the bright end, which occurs at fainter luminosities in lower-density regions. This, in turn, is simply a reflection of the fact that most bright galaxies reside in massive haloes.

Our CLF model also predicts a pronounced difference for the environment dependence of the LFs of early- and late-type galaxies. As shown in Fig. 4, the *shape* of the LF of early-type galaxies depends rather strongly on δ. For the late-type galaxies, however, no such pronounced shape dependence is predicted. Once again, this behaviour is easy to understand from the conditional halo mass function and the CLF: many of the fainter early-types actually reside in clusters (see Paper II), the abundance of which depends strongly on δ. The majority of the faint late-type galaxies, on the other hand, resides in relatively low-mass haloes, for which the shape of the conditional halo mass function is roughly independent of environment (cf. Fig. 2).

To quantify further how the LF depends on the mean density of the environment, we fit each of the LFs by a Schechter form. For most of our discussion, we only fit over the luminosity range $L \geqslant 10^9\ h^{-2}$ $L_\odot$ ($M_{b_J} - 5 \log h \lesssim -17.2$). In real redshift surveys, such as the 2dFGRS, galaxies fainter than this are observed only within a relatively small local volume, making it difficult to study their large-scale environment dependencies. As shown in Figs 3 and 4, the Schechter function provides, in general, a reasonable fit to the LF over a large range in luminosity. This is not a trivial result, as the shape of the CLF varies significantly with halo mass and the conditional mass function at the high-mass end changes significantly with δ.

The left-hand panel of Fig. 5 shows the characteristic luminosity L^* and the faint-end slope α as functions of δ. In all cases, the characteristic luminosity increases with δ, reflecting the fact that massive haloes, which host bright galaxies, are preferentially located in high-density regions. The increase is only moderate: for the total sample, it is about 1 mag from the lowest to the highest densities probed. The increase is more significant for early-type galaxies than for late-type galaxies. For late-type galaxies, the increase becomes insignificant for $\delta \gtrsim 1$.

For the total population, the faint-end slope α is roughly a constant, with a value of about -1.1. The faint-end slope is also quite independent of δ for late-type galaxies, with $\alpha \sim -1.25$. In contrast, the faint-end slope for early-type galaxies changes from
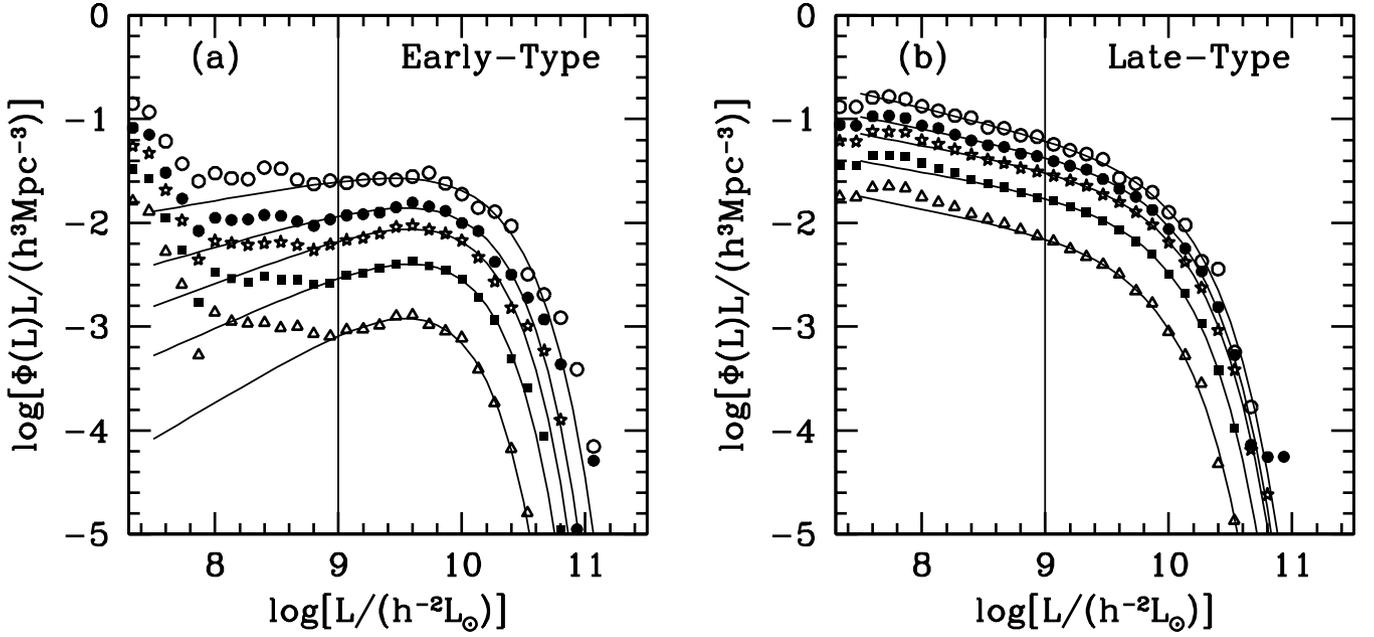
Figure 4. The same as Fig. 3, but for (a) early-type and (b) late-type galaxies. Solid curves correspond to the best-fitting Schechter functions, fit over the range $L \geqslant 10^9 \, h^{-2} \, \mathrm{L_\odot}$.
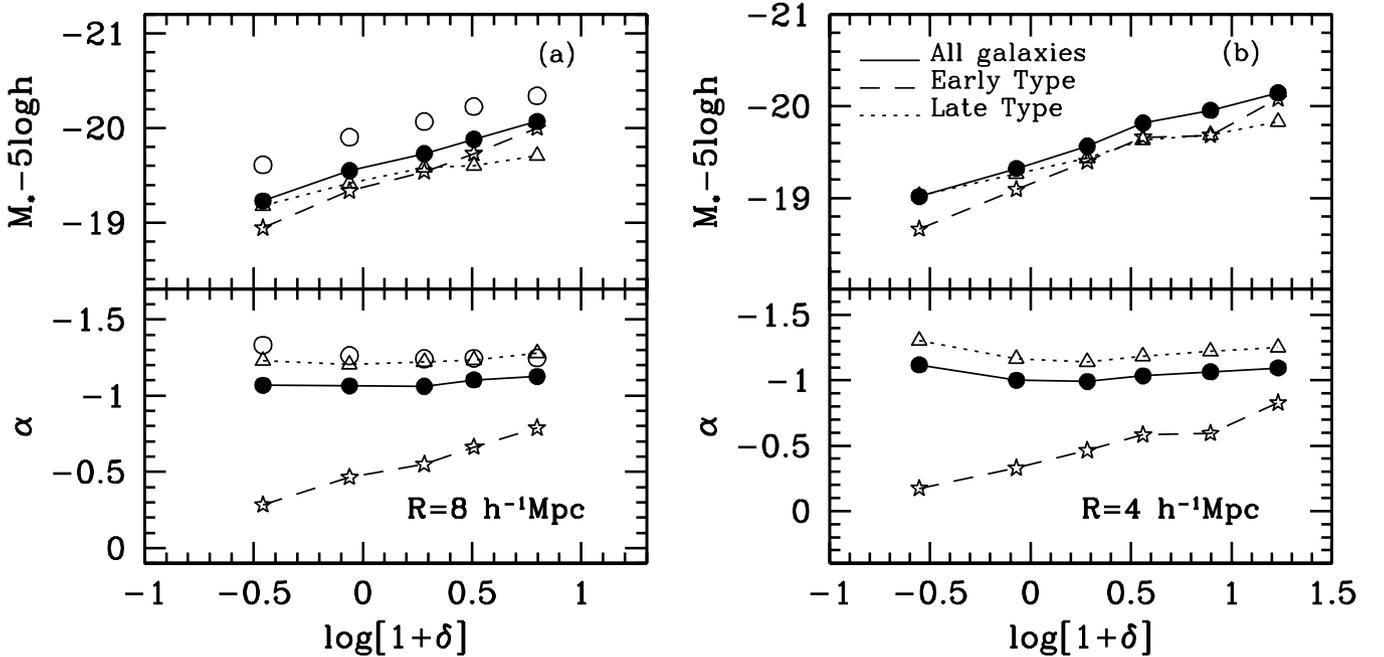

Figure 5. The characteristic luminosity and faint-end slope α as a function of δ, defined as the mean overdensity within individual spheres of radius $R = 8 \, h^{-1}$ Mpc (left-hand panel) and $R = 4 \, h^{-1}$ Mpc (right-hand panel). Symbols connected with lines are results of the fit over the luminosity range $L \geqslant 10^9 \, h^{-2} \, \mathrm{L_\odot}$ for the total (solid line), early-type (dashed line) and late-type (dotted line) samples. For comparison, the open circles in the left-hand panel show the results for the total sample when fitting over the more extended luminosity range $L \geqslant 10^{7.5} \, h^{-2} \, \mathrm{L_\odot}$.

$\alpha \sim -0.3$ for low-density regions to $\alpha \sim -0.8$ for $\delta \sim 10$. As mentioned above, this is mainly due to the fact that a large number of relatively faint early types reside in massive haloes which have mass functions depending strongly on δ.

If we fit the LF over the entire range with $L \gtrsim 10^{7.5} \, h^{-2} \, \mathrm{L_\odot}$ ($M_{b_J} - 5 \log h \lesssim -13.5$), the faint-end slope becomes steeper for low-density regions (cf. open and solid circles in left-hand panel of Fig. 5). Note that, in this case, the Schechter function is no longer

a good fit (see Fig. 3) for low-density regions; the faint-end slope is much steeper than that of the extrapolation from the LF at the brighter end. This departure starts at $L \sim 10^9 \, h^{-2} \, \mathrm{L_\odot}$ and is more significant for early-type galaxies.

We have also made similar analyses for spherical volumes with a radius of $4 \, h^{-1}$ Mpc, the results of which are shown in the right-hand panel of Fig. 5. A noticeable difference with using volumes of $8 \, h^{-1}$ Mpc radius is that the characteristic luminosity increases faster with

δ. The reason is that the conditional mass function at the high-mass end reveals a stronger dependence on δ for smaller radius R (see Fig. 2).

4 PREDICTIONS FOR OBSERVATIONAL TESTS

So far, we have investigated how the galaxy LF depends on the mass density averaged over spherical volumes of $8\ h^{-1}$ Mpc radius. Unfortunately, it is not easy observationally to obtain accurate measures for the mass density field in the Universe. Therefore, in order to facilitate an observational test of the predictions presented above, we need to find a quantity that is (i) easy to derive from observations and (ii) that can be used to rank the mass density.

When averaged within a large volume, the *number* density, δ_g, of galaxies (with luminosities above some value) and the luminosity density, δ_L, are both expected to be correlated with the underlying mass density. Such relations can be derived directly from the simulated catalogues constructed with the CLF (Yang et al. 2003b). Fig. 6 shows the results. As one can see, there is a tight correlation between the luminosity overdensity δ_L and mass overdensity δ. Here, δ_L is calculated using all galaxies with $L \geqslant L_{\min} = 10^7\ h^{-2}$ $L_\odot$, but it is not sensitive to this lower limit as long as $L_{\min} \lesssim 10^9\ h^{-2}$ $L_\odot$. Thus the luminosity density can be used to rank the mass density. The use of galaxy *number* density is trickier, because the scatter is quite large for low-density volumes (for example, δ_g, here defined by all galaxies with $L \geqslant 10^9\ h^{-2}\ L_\odot$, becomes zero at $\delta < -0.8$ in the right-hand panel of Fig. 6) and because it depends on the luminosity range used in defining the galaxy overdensity δ_g (because the number density of galaxies is dominated by the faint ones).

In order to show that δ_L can be used to rank δ, we first fit the mean ρ_L–ρ relation by the following function:

$$y = Ae^{-x_*}x^\beta e^{x_*/x}, \tag{15}$$

where $x = 1 + \delta$, $y = 1 + \delta_L$, and A, x_* and β are fitting parameters. For high-density cells ($x \gg x_*$), $y \propto x^\beta$, whereas for $x \ll x_*$, y decreases exponentially with decreasing x. For $R = 8\ h^{-1}$ Mpc, we obtain $A = 1.0203$, $x_* = -0.3053$ and $\beta = 0.8035$. We then use this mean relation to convert the distribution function of the mass density into a distribution function for the luminosity density, and compare it with the luminosity-density distribution function derived directly from the simulation. The result is shown in Fig. 7. Clearly, the luminosity-density distribution function is recovered quite accurately with the mean relation (15), suggesting that the luminosity density can be used to represent the mass density.

Fig. 8 shows how L^* and α change with the luminosity density. The results are similar to those shown in Fig. 5, except that the range of δ_L is stretched at the low-density end relative to δ, because of the non-linear relationship between δ_L and δ. As comparison, we also show L^* and α as functions of δ_g, where δ_g is based on the number of galaxies with $L \geqslant 10^9\ h^{-2}\ L_\odot$ (Fig. 9). With such a luminosity limit, the results based on δ_g are very close to those based on δ_L.

5 DISCUSSION

We have shown that the halo-occupation model, which assumes that the luminosity distribution in a dark halo only depends on its mass, makes specific predictions about how the galaxy LF changes with large-scale environment. The model predicts that the LFs for relatively bright galaxies can be fit reasonably well by a Schechter function, independent of environment. In all cases, the characteristic luminosity $L*$ increases with local mass density. For late-type galaxies, the faint-end slope is quite independent of large-scale environment, whereas for early-types, the value of α changes from ~ 0 in low-density regions to ~ -1 in high-density regions. The predicted LF for low-density regions shows significant departure from the Schechter form at $L \lesssim 10^9\ h^{-2}\ L_\odot$, and this departure is more significant for early-type galaxies. All these predictions have simple
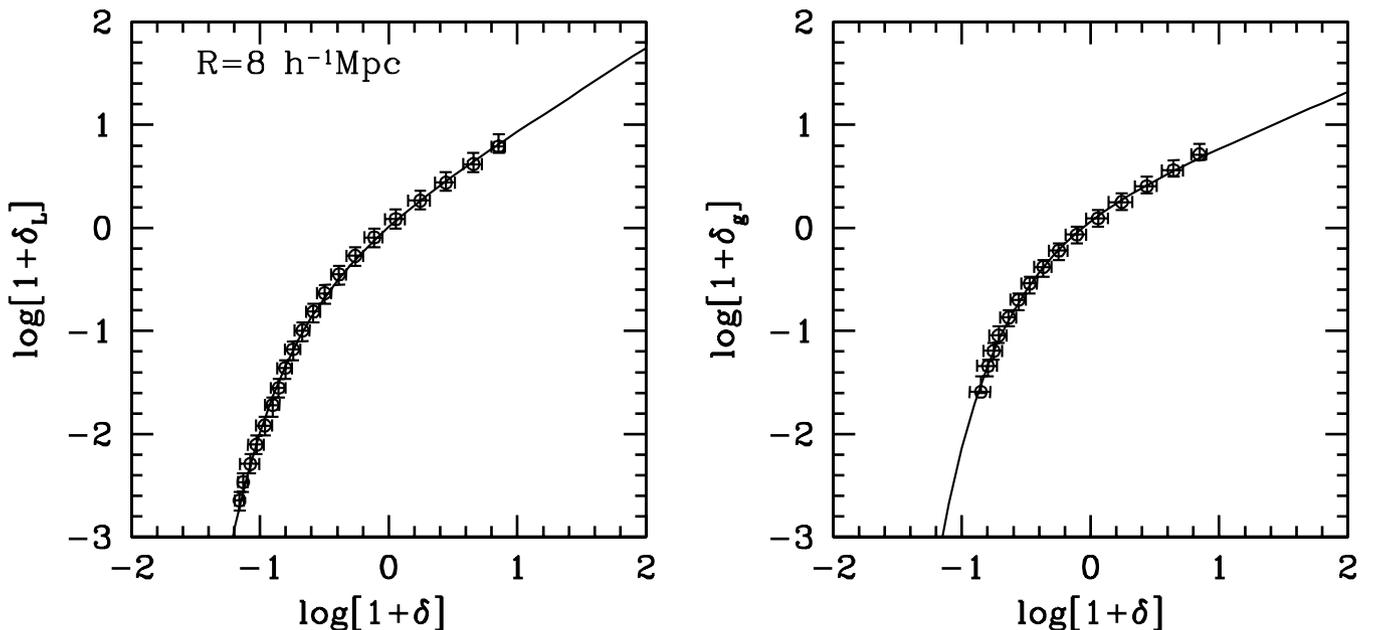

Figure 6. The left-hand panel shows the relation between luminosity density (δ_L, calculated using all galaxies resolved in the simulation) and mass density (δ), whereas the right-hand panel shows the galaxy number density (δ_g, calculated using galaxies with luminosity $L \geqslant 10^9\ h^{-2}\ L_\odot$). All quantities are the averages within a sphere of radius $R = 8\ h^{-1}$ Mpc, and are normalized to the corresponding mean densities of the Universe. The curves show the fits to the relations. Error bars for δ_L and δ_g represent the ranges of the quantities, whereas error bars for δ are 1σ standard deviations. Note that below a certain value of δ, $\log(1 + \delta_g)$ becomes $-\infty$, whereas $\log(1 + \delta_L)$ is still finite.
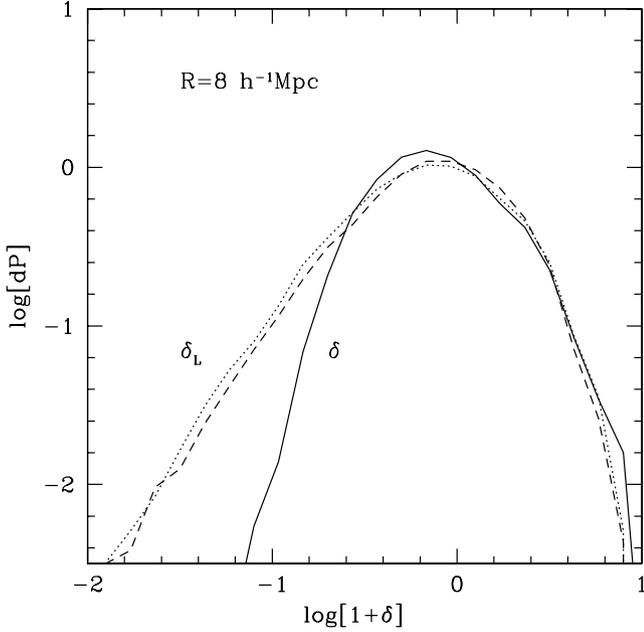
Figure 7. The solid and dashed curves show the distribution functions of the mass overdensity δ and of the luminosity density δ_L, respectively. The dotted curve shows the conversion of the distribution of mass density to the distribution of luminosity density using the mean δ_L–δ relation shown in Fig. 6.
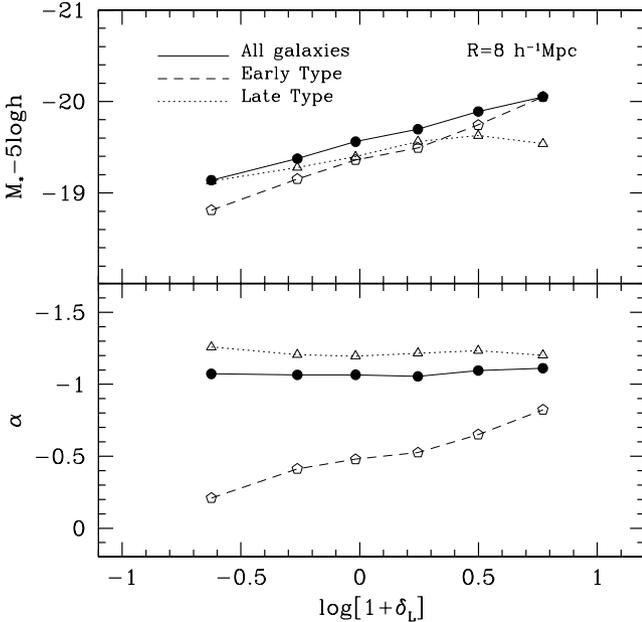

Figure 8. The characteristic magnitude, M_*, and the faint-end slope, α, of the best-fitting Schechter function as functions of δ_L. The results are shown for the total, early-type and late-type samples, as indicated. Schechter functions are fit to the LFs over the range $L \geqslant 10^9 \; h^{-2} \; L_\odot$.

explanations based on the change of halo mass function with large-scale environment, and the change of halo occupation with halo mass.

We have also shown that the luminosity density is tightly correlated with the mass density on large scales. Thus, our predictions can be checked using large galaxy redshift surveys. At the moment,
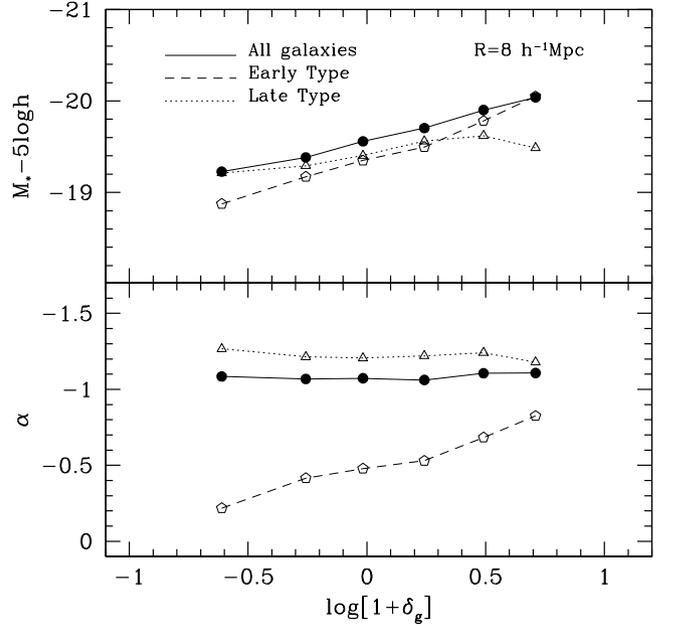

Figure 9. The same as Fig. 8, but as a function of δ_g, the overdensity (in number) of galaxies with $L \geqslant 10^9 \; h^{-2} \; L_\odot$.

the study of the dependence of galaxy LF on local environment has mainly focused on comparing the LF of cluster galaxies with that of field galaxies (see, for example, De Propris et al. 2003, and references therein). More related to the model predictions presented here are the analyses made by Hütsi et al. (2002) and Bromley et al. (1998). Hütsi et al. estimated galaxy LFs in spherical volumes with a radius $10 \; h^{-1}$ Mpc (in redshift space) within which the overdensities of galaxy number are, respectively, $\delta_g < 0$, $0 < \delta_g < 1$, and $\delta_g > 1$, and found that the faint-end slope α is about -1.1 for all the three cases, but that the characteristic luminosity brightens by about 0.4 mag from the lowest-density sample to the highest-density sample. These results are consistent with our model prediction. Bromley et al. found that the faint-end slope of the LF of early-type galaxies (defined according to spectral type) depends strongly on local density, with α increasing from ~ -0.4 in high density regions to ~ 0.2 in low-density regions. This trend is also consistent with our model prediction. Unfortunately, current observational results are not yet sufficiently accurate to give a stringent constraint on the model. The situation will soon change. With the use of large redshift surveys of galaxies, such as the 2dFGRS and SDSS,[1] one can estimate to high accuracy the galaxy luminosity functions in regions of different luminosity densities or galaxy number densities (Croton et al., in preparation), facilitating an accurate comparison between model and observations.

If our model prediction agrees in detail with observational data, it will add strong support to the assumptions made in the theory: the 'concordance' cosmology (which determines the properties of the halo population) and that galaxy properties only depend on halo mass. If we assume that the halo population in the real Universe is not very different from that predicted by the 'concordance' cosmology, any significant difference between our model prediction and

---

[1] During the final stages of this project, Hoyle et al. (2003) published a paper based on SDSS data that addresses the environment-dependence of the LF. Their results are qualitatively in good agreement with our predictions, though we delay a more detailed comparison to a future paper.

observation would have important implications for the formation of galaxies in the cosmic density field. For example, the prediction that the faint-end slope of the LF should not depend significantly on large-scale environment is due to the fact that most of the faint galaxies in our CLF model are in low-mass haloes. A significant discrepancy between model prediction and observation would therefore require a CLF model in which many faint galaxies are in massive haloes. This change of CLF is, however, strongly constrained by the observed weak clustering of faint galaxies. Thus, any significant discrepancy would strongly indicate the assumption that the galaxy properties only depend on halo mass is incorrect, invalidating the whole halo-occupation approach. The other prediction of the model, that the characteristic luminosity increases mildly with local density, is due to the fact that, in our CLF model, bright galaxies are preferentially found in massive haloes. Here, any discrepancy with observational data would therefore require a change in the fraction of bright galaxies in massive haloes. Such change will lead to a change in the correlation length as a function of luminosity, and is subject to stringent observational constraints. As mentioned above, the other CLF models we have obtained give very similar results, and so any significant discrepancy would mean that either galaxy properties depend significantly on other properties of haloes in addition to the mass, or our parametrization of the CLF is not sufficiently general. As discussed in Paper I, our parametrization is motivated by physical considerations, and is quite general as long as the CLF is assumed to be a smooth function of halo mass. Thus, should a sigificant change in the CLF be required by the observation, it would have a significant impact on our understanding of galaxy formation in dark matter haloes.

As far as an accurate comparison with observation is concerned, there are several effects to be taken into account. The first is redshift distortion. Because bright galaxies in massive clusters are expected to have large velocity dispersion, some of these galaxies may appear in 'low-density' regions in redshift space, weakening the dependence on δ. This effect was seen in our experiment where δ was defined in redshift space. The second is concerned with the definition of overdensity. In a magnitude-limited sample, volumes at large distances from us contain only bright galaxies, and so the estimate of the overdensity in such a cell has to rely on a small number of bright galaxies. Because the shape of the LF changes with δ, the correction of the incompleteness due to the magnitude limit in individual volumes must take this effect into account. Finally, since the Schechter function is not a perfect model, the fitting parameters depend on the luminosity *range* used for the fit. All these effects can be taken into account properly with the use of mock catalogues by applying the same analyses to both the simulated and observed samples. We plan to present such a detailed comparison with observational data in a forthcoming paper.

It is also interesting to compare the predictions presented here, based on the CLF, with those based on semi-analytical models for galaxy formation (e.g. Kauffmann et al. 1999; Somerville & Primack 1999; Benson et al. 2002; Mathis et al. 2002). Mathis et al. (2002) have shown that the characteristic luminosity of the galaxy LF in their semi-analytical model increases progressively from low-density to high-density environments while the faint-end slope becomes slightly shallower. These results are in qualitative agreement with our predictions presented here. As already emphasized in Paper II, this suggests that the halo-occupation statistics as described by our CLF nicely fit within the standard framework of galaxy formation.

REFERENCES

Benson A. J., 2001, MNRAS, 325, 1039
Benson A. J., Lacey C. G., Baugh C. M., Cole S., Frenk C. S., 2002, MNRAS, 333, 156
Berlind A. A., Weinberg D. H., 2002, ApJ, 575, 587
Berlind A. A. et al., 2003, ApJ, 593, 1
Bullock J. S., Wechsler R. H., Somerville R. S., 2002, MNRAS, 329, 246
Bromley B. C., Press W. H., Lin H., Kirshner R. P., 1998, ApJ, 505, 25B
Cole S., Kaiser N., 1989, MNRAS, 237, 1127
Cole S., Aragon-Salamanca A., Frenk C. S., Navarro J. F., Zepf S. E., 1994, MNRAS, 271, 781
Colless M. et al., 2001, MNRAS, 328, 1039
De Propris R. et al., 2003, MNRAS, 342, 725
Gottloeber S., Lokas E., Klypin A., Hoffman Y., 2003, MNRAS, 344, 715
Hoyle F., Rojas R. R., Vogeley M. S., Brinkmann J., 2003, ApJ, submitted (astro-ph/0309728)
Hütsi G., Einasto J., Tucker D. L., Saar E., Einasto M., Müller V., Heinämäki P., Allam S. S., 2002, A&A, submitted (astro-ph/0212327, submitted to A&A)
Jing Y. P., Mo H. J., Börner G., 1998, ApJ, 494, 1
Jing Y. P., Suto Y., 2002, ApJ, 574, 538
Kang X., Jing Y. P., Mo H. J., Börner G., 2002, MNRAS, 336, 892
Kauffmann G., White S. D. M., Guiderdoni B., 1993, MNRAS, 264, 201
Kauffmann G., Colberg J. M., Diaferio A., White S. D. M., 1999, MNRAS, 303, 188
Kravtsov A. V., Berlind A. A., Wechsler R. H., Klypin A. A., Gottloeber A., Allgood B., Primack J. R., 2003, ApJ, submitted (astro-ph/0308519)
Lemson G., Kauffmann G., 1999, MNRAS, 302, 111
Magliocchetti M., Porciani C., 2003, preprint (astro-ph/0304003)
Mathis H., White S. D. M., 2002, MNRAS, 337, 1193
Mathis H., Lemson G., Springel V., Kauffmann G., White S. D. M., Eldar A., Dekel A., 2002, MNRAS, 333, 739
Mo H. J., White S. D. M., 1996, MNRAS, 282, 347
Peacock J. A., Smith R. E., 2000, MNRAS, 318, 1144
Scoccimarro R., Sheth R. K., Hui L., Jain B., 2001, ApJ, 546, 20
Scranton R., 2002, MNRAS, 332, 697
Seljak U., 2000, MNRAS, 318, 203
Sheth R. K., Tormen G., 1999, MNRAS, 308, 119
Sheth R. K., Tormen G., 2002, MNRAS, 329, 61
Sheth R. K., Mo H. J., Tormen G., 2001, MNRAS, 323, 1
Somerville R. S., Primack J. R., 1999, MNRAS, 310, 1087
Spergel D. N. et al., 2003, preprint (astro-ph/0302209)
van den Bosch F. C., Yang X. H., Mo H. J., 2003a, MNRAS, 340, 771 (Paper II)
van den Bosch F. C., Mo H. J., Yang X. H., 2003b, MNRAS, 345, 923
White S. D. M., Rees M. J., 1978, MNRAS, 183, 341
Yan R., Madgwick D. S., White M., 2003, preprint (astro-ph/0307248)
Yang X. H., Mo H. J., van den Bosch F. C., 2003a, MNRAS, 339, 1057 (Paper I)
Yang X. H., Mo H. J., Jing Y. P., van den Bosch F. C., Chu Y. Q., 2003b, MNRAS, in press (astro-ph/0303524)
York D. et al., 2000, AJ, 120, 1579
Zehavi I. et al., 2003, preprint (astro-ph/0301280)
Zheng Z., Tinker J. L., Weinberg D. H., Berlind A. A., 2002, ApJ, 575, 617

This paper has been typeset from a TEX/LATEX file prepared by the author.